

Charged analogues of a singularity-free anisotropic compact star under linear $f(Q)$ - action

Debadri Bhattacharjee^a, Pradip Kumar Chattopadhyay^a

^a*IUCAA Centre for Astronomy Research and Development (ICARD), Department of Physics, Coochbehar Panchanan Barma University, Vivekananda Street, District: Coochbehar, Pin: 736101, West Bengal, India.,*

Abstract

This study simulates the characteristics of spherically symmetric, anisotropic compact stellar bodies with electrical charge within the context of the $f(Q)$ theory of gravity. Employing the Krori-Barua metric ansatz (K.D. Krori, J. Barua, J. Phys. A: Math. Gen. 8 (1975) 508) along with a linear form of $f(Q)$ model, *viz.*, $f(Q) = \alpha_0 + \alpha_1 Q$, we obtain a tractable set of exact relativistic solutions of the field equations. A specific form of charge ($q = q_0 r^3$) is considered here for the present analysis. Using the data sets of ρ and p_r along with the method of curve fitting, we have obtained the best fit equation of state in the model, which is incorporated in the numerical solutions of the TOV equations to determine the maximum mass and radius in this scenario. With increasing charge intensity (q_0) from 0.0002 to 0.0006, the maximum mass ranges from $2.838 - 2.869 M_\odot$, and the corresponding radii range from $12.0039 - 12.0822 \text{ Km}$. Moreover, the predicted radii of some recently observed pulsars and GW 190814 show that our model also complies with the estimated radii based on the observational results. Our model is found to satisfy all the characteristic features, such as behaviour of matter variables, causality condition, energy constraints and stability criteria, which are pertinent in the context of a stable stellar configuration to emerge as a viable and physically acceptable stellar model in the framework of $f(Q)$ gravity.

Keywords: $f(Q)$ gravity, Charge, Equation of state, Maximum mass, Exact solution

1. Introduction

In 1912, Einstein's exploration of static gravitational fields led him to a daring proposition. A straightforward application of his principle of equivalence, combined with the fundamental outcomes of special relativity, implied that the gravitational field is characterised by the metric tensor. He hypothesised that this holds true even beyond the static limit and this set him on a three-year quest that concluded in November 1915 with the formulation of the field equations of his General Theory of Relativity (GR). In the later years, GR has solved many persistent mysteries pervading in astrophysics and cosmology. Despite being remarkably successful, GR has faced significant challenges when confronted with astrophysical and cosmological observational results. For instance, numerous distinct cosmological studies suggest that our universe is undergoing an accelerated expansion [1, 2, 3], the phenomenon of dark energy and dark matter, which are essential in galactic dynamics, as well as the accelerated expansion of the universe, etc., are not adequately explained within the framework of GR without introducing exotic forms of matter and energy. Additionally, GR predicts singularities, such as those at the centres of black holes and the Big Bang, where the laws of physics break down. These singularities indicate a need for a more comprehensive theory that can be seamlessly integrated with quantum mechanics for a deeper understanding at the minute level. In this context, modified theories of gravity offer an intricate way to address these challenges by extending the geometrical and dynamical foundations of GR, potentially offering alternative explanations for these enigmatic phenomena and providing a more complete understanding of the universe.

Soon after the advent of GR, Weyl [4] imposed the first modifications on it by introducing higher order invariants to the Einstein-Hilbert action to unify electromagnetism and gravitation. Later, GR was modified by two types of geometrical extensions, *viz.*,

- extensions based on curvature, such as the $f(R)$, $f(T)$, $f(R, T)$, etc., theories of gravity.

- extensions based on torsion and non-metricity [5] such as the $f(Q)$ theory of gravity.

Such torsion and non-metricity based theories of gravity, which are equivalent to GR, are termed the Teleparallel Equivalent of General Relativity (TEGR) [6, 7] and the Symmetric Teleparallel Equivalent of General Relativity (STEGR) [9, 10]. In the context of flat space-time with torsion, the TEGR is formulated using the tetrads and spin connections as the primary variables. The constraints imposed by the nullification of the curvature and non-metricity tensor restrict the spin connection. This allows for the adoption of the Weitzenböck connection, where all elements of the spin connections are eliminated, leaving only the tetrad components as the fundamental entities. This selection is interpreted as a gauge choice within the framework of TEGR. It is noteworthy that this choice does not influence the physical implications of the theory, as any other selection compatible with the teleparallelism constraint would yield the same action, barring a surface term. On the other hand, in the framework of STEGR, it is the non-metricity that characterises gravity, as opposed to curvature and torsion. Within the constraints of teleparallelism, a particular gauge, known as the coincidence gauge, can be selected in this theory. This gauge selection sets the metric tensor as the sole fundamental variable. An additional extension of the STEGR is the $f(Q)$ gravity theory, which bears a significant resemblance to the $f(R)$ gravity theory [9, 11]. Within the general formalism of $f(Q)$ gravity, Hohmann et al. [12] studied the potential polarisation and the velocity of propagation of gravitational waves in Minkowski space. Subsequently, Soudi et al. [13] showed that gravitational wave polarisation has an important impact on the strong-field nature of theories of gravity. $f(Q)$ theory has been utilised in a wide range of topics, including late-time acceleration [14], black holes [15, 16], bouncing [17], evolution of the growth index in the context of matter fluctuations [18], and $f(Q)$ parametrisation to integrate the observational constraints [19]. A detailed review of $f(Q)$ formalism has been described in Ref. [20]. In addition, several aspects of $f(Q)$ gravity have been described in Refs. [21, 22, 23, 24, 25].

In the astrophysical context, the study of compact objects within the framework of modified gravity is essential for advancing our understanding of fundamental physics. Compact objects such as black holes and neutron stars provide extreme environments where the effects of gravity are exceptionally strong, offering unique testing grounds for theories that extend beyond GR. These objects can reveal discrepancies between observed phenomena and theoretical predictions, shedding light on potential modifications to our current gravitational models. Recently, a substantial volume of data from pulsars and gravitational wave (GW) events has been collected and scrutinised by numerous researchers. This comprehensive analysis has led to precise predictions of several physical parameters pertaining to such celestial bodies. By utilising the Shapiro delay [26] an accurate determination of the mass of millisecond pulsar PSR J0740+6620 resulted to be $2.14^{+0.10}_{-0.09}$. In addition to this, it is postulated that there could be a few compact celestial bodies that possess masses exceeding that of PSR J0740+6620 [26], particularly within the cluster of interacting systems. The occurrence of gravitational wave event, referred to as GW 190814, has indicated that the associated star boasts a mass ranging from 2.5 to 2.67 M_{\odot} , with a confidence level of 90%. It is currently unclear whether this component represents an extremely massive compact star or a lightweight black hole. If the former is true, it becomes imperative to introduce a novel concept into the theoretical framework to extend the maximum mass range to account for such elevated mass values. This kind of formalism would be crucial for investigating the internal structure of dense matter beyond saturation density.

The pressure anisotropy within a compact celestial body can be attributed to various factors. One potential cause is the existence of a type 3A superfluid within the solid core of these objects [27]. Due to the nature of fermions, nucleons cannot occupy the same energy state simultaneously, a principle known as the Pauli exclusion principle. Additionally, strong repulsive interactions between nucleons occur within very short ranges. These repulsive forces aid in counteracting gravitational collapse within a neutron star. However, this scenario changes when temperatures are extremely low, leading to the formation of Cooper pairs [28] of nucleons, which essentially behave as bosons. Consequently, at very low temperatures, nucleons exhibit collective behaviour on a large scale. These nucleon condensates, analogous to Helium-3, can flow without any viscosity. Within a neutron star, the high-pressure region effectively raises the critical temperature for Cooper pair formation, allowing for the occurrence of nuclear superfluidity even at temperatures on the order of a billion degrees. There could be three distinct types of superfluids present within the core of a neutron star [29]. Other potential sources of anisotropy in compact objects could include phase transitions [30], pion condensation [31], slow rotation and viscosity [32].

Rosseland [33] was the first to propose that a star could be composed of a substantial number of electrons and positive ions. Given their extremely high kinetic energy, electrons have a higher likelihood of escaping from the star compared to positive ions. As a result, a star can possess a considerable amount of net positive charge. This process

persists until the internal electric field prevents further electron escape [34]. The Einstein Field Equations (EFE), when considering an electric field, are crucial for examining the properties of neutron stars, quark stars, gravastars, black holes, and other entities in the realm of relativistic astrophysics. This is because the electric field significantly influences the overall properties of such compact objects. In his study, Ivanov [35] showed that one of the most important prerequisites for obtaining a singularity-free perfect fluid distribution is the presence of non-vanishing net charge. While arguing on the results of Hoyle and Narlikar [36] about the collapse of a large mass of gas into singularity, Bonnor [37] showed that electric repulsion can counterbalance the gravitational collapse of a spherical body to achieve an equilibrium configuration. Stettner [38] showed that a spherical structure with a net surface charge is more stable than a structure with a uniform density. Krasinski [39] demonstrated that preventing the gravitational collapse of spherically distributed matter into a point singularity necessitates the presence of a net charge. Through a generalisation of the Oppenheimer–Volkoff equation, Bekenstein [40] conducted a qualitative assessment of the stability of spheres composed of charged fluid. Over the years, several researchers have addressed the impact of charge on compact stellar structures [41, 42, 43, 44, 45, 46, 47, 48, 49].

Recently, the $f(Q)$ theory has garnered a significant amount of attention from researchers worldwide. In the astrophysical scenario, it has provided new insights into compact stellar structures. In the context of charged configurations, Kaur et al. presented a charged $f(Q)$ solution to study an anisotropic fluid distribution using the Vaidya-Tikekar metric ansatz. Maurya et al. [51] used an interesting approach of gravitational decoupling into the $f(Q)$ theory to study the constraining factors of mass and radii of the lighter component of GW190814 and other self-bound strange stars. Errehymy et al. [52] studied a singularity-free charged strange star model in the framework of $f(Q)$ gravity. Furthermore, Lohakare et al. [53] investigated the effects of gravitational decoupling on the maximum mass and stability of charged strange stars. In addition, several authors have included $f(Q)$ theory in their analysis of a stable stellar structure [54, 55, 56, 57].

In the present manuscript, we have investigated the impact of charge on the structure of a singularity-free compact star model within the framework of linear $f(Q)$ action. The advantage of $f(Q)$ gravity lies in its ability to derive the equations of GR without the necessity of employing the affine connection, thereby enhancing the inertial gravitational acceleration. This intriguing aspect coupled with the charged configuration reveals interesting stellar properties. The rest of the paper is organised in the following manner: Section 2 demonstrates the fundamental ground work of $f(Q)$ theory in the presence of charge. Section 3 addresses the formulation and solution of the Einstein-Maxwell equations in the framework of $f(Q)$ gravity. The analytical expressions of the thermodynamic quantities such as energy density (ρ), radial (p_r) and tangential (p_t) pressures are obtained in this section. The effects of $f(Q)$ parameters on the boundary conditions are described in Section 4. Section 5 deals with the physical characteristic features of the model along with the determination of the maximum mass and radius, causality condition and energy conditions. The necessary stability criteria are addressed in Section 6. Finally, we conclude by summarising the major findings of the paper in Section 7.

2. Fundamentals of $f(Q)$ gravity in the presence of charge

In this framework of symmetric teleparallel $f(Q)$ gravity, the gravitational action integral in the presence of an electromagnetic field is expressed as [9, 58]:

$$\mathfrak{S} = \int \sqrt{-g} d^4x \left[\frac{1}{2} f(Q) + \lambda_l^{kij} R_{kij}^l + \tau_k^{ij} T_{ij}^k + \mathfrak{L}_m + \mathfrak{L}_q \right], \quad (1)$$

where, g defines the determinant of the fundamental metric tensor g_{ij} , i.e., $g = |g_{ij}|$, $f(Q)$ is a function of non-metricity Q , λ_l^{kij} and τ_k^{ij} are two Lagrangian multipliers, R_{kij}^l and T_{ij}^k are the Riemann tensor and torsion tensor, respectively, and L_m and L_q describe the Lagrangian density of matter and electromagnetic charge, respectively. Using affine connections (Γ_{ij}^k), the non-metricity is expressed as:

$$Q_{kij} = \nabla_k g_{ij} = \delta_k g_{ij} - \Gamma_{ij}^l g_{lj} - \Gamma_{ik}^l g_{jl}, \quad (2)$$

where, ∇_k is the covariant derivative. Again, the affine connection can be sub-divided into three components in the following way:

$$\Gamma_{ij}^k = \epsilon_{ij}^k + K_{ij}^k + L_{ij}^k. \quad (3)$$

In the above expression,

- ϵ_{ij}^k is the Levi-Civita connection which, with the help of the fundamental metric tensor g_{ij} , is defined as:

$$\epsilon_{ij}^k = \frac{1}{2} g^{kl} \left(\partial_i g_{lj} + \partial_j g_{il} - \partial_l g_{ij} \right). \quad (4)$$

- K_{ij}^k describes the contorsion and is expressed as:

$$K_{ij}^k = \frac{1}{2} T_{ij}^k + T_{(i}{}^k{}_{j)}. \quad (5)$$

In the STEGR, the contorsion (K_{ij}^k) physically represents the anti-symmetric part of the affine connection, which is written in the following form: $T_{ij}^k = 2\Gamma_{[ij]}^k = \Gamma_{ij}^k - \Gamma_{ji}^k$.

- The final term on the right hand side of Eq. (3) represents the deformation and is expressed as:

$$L_{ij}^k = \frac{1}{2} Q_{ij}^k + Q_{(i}{}^k{}_{j)}. \quad (6)$$

The superpotential associated with the non-metricity is described as,

$$P^{kij} = -\frac{1}{4} Q^{kij} + \frac{1}{2} Q^{(ij)k} + \frac{1}{4} (Q^k - \tilde{Q}^k) g^{ij} - \frac{1}{4} \delta^{k(i} Q_{j)}, \quad (7)$$

where, Q^k and \tilde{Q}^k define the independent traces of Q_{kij} as:

$$Q_k \equiv Q_{ki}^i, \quad \tilde{Q}^k = Q_i^{ki}. \quad (8)$$

Ultimately, the non-metricity scalar is expressed by the following equation:

$$Q = -g^{ij} \left(L_{ij}^k L_{ik}^l - L_{il}^l L_{ij}^k \right) = -Q_{kij} P^{kij}. \quad (9)$$

Due to the absence of torsion and curvature, the affine connection can be effectively characterised by a tractable set of functions described as:

$$\Gamma_{ij}^k = \left(\frac{\partial x^k}{\partial \chi^l} \right) \partial_i \partial_j \chi^l, \quad (10)$$

where, in the context of a general co-ordinate transformation, we consider arbitrary spacetime position functions denoted by χ^l . Notably, we always have the flexibility of choosing the co-ordinate of the form $\chi^l = \chi^l(x^i)$. Following the study of Jiménez et al. [9], the generality of affine connection, i.e., $\Gamma_{ij}^k = 0$, is termed the coincident gauge property. Hence, the covariant derivatives in the coincident gauge reduce to ordinary derivatives in the standard GR, and consequently, the non-metricity formalism of Eq. (3) can be simplified as:

$$Q_{kij} = \partial_k g_{ij}. \quad (11)$$

Now, we obtain the tractable set of gravitational field equations by varying the Einstein-Hilbert action as written in Eq. (1) with respect to the metric tensor g_{ij} in the form:

$$\frac{2}{\sqrt{-g}} \nabla_k \left(\sqrt{-g} f_Q P_{ij}^k \right) + \frac{1}{2} g_{ij} f + f_Q \left(P_{ikl} Q_j^{kl} - 2 Q_{kli} P_j^{kl} \right) = - \left(T_{ij} + E_{ij} \right), \quad (12)$$

where, $f_Q = \frac{\partial f}{\partial Q}$, T_{ij} and E_{ij} respectively represent the energy-momentum tensors of the matter and electromagnetic contribution. In a generalised way, we can describe T_{ij} and E_{ij} in the following forms:

$$T_{ij} = -\frac{2}{\sqrt{-g}} \frac{\delta(\sqrt{-g} \mathfrak{L}_m)}{\delta g^{ij}} \quad \text{and} \quad E_{ij} = -\frac{2}{\sqrt{-g}} \frac{\delta(\sqrt{-g} \mathfrak{L}_q)}{\delta g^{ij}}. \quad (13)$$

Moreover, the variation of action with respect to the affine connection yields,

$$\nabla_i \nabla_j \left(\sqrt{-g} f_Q P_{ij}^k - \frac{1}{2} \frac{\delta \mathcal{L}_m}{\delta \Gamma_{ij}^k} \right) = 0, \quad (14)$$

where, the second term in Eq. (14) defines the tensor density of the hyper momentum. Imposing the relation $\nabla_i \nabla_j (H_{ij}^k) = 0$, Eq. (14) reduces to $\nabla_i \nabla_j (\sqrt{-g} f_Q P_{ij}^k) = 0$.

3. Mathematical formalism: $f(Q)$ gravity and Einstein-Maxwell field equations

In this paper, we investigating a novel generalised approach to charged compact star modeling in the framework of the $f(Q)$ theory of gravity. Within the realm of gravitational theories, the concept of static spherically symmetric spacetime serves as a foundational assumption, offering valuable insights into various aspects of astrophysical phenomena. Keeping this in mind, we have considered a static spherically symmetric spacetime for the analysis of the present paper. Now, in the static spherically symmetric curvature co-ordinate space (t, r, θ, ϕ) , the line element is expressed as:

$$ds^2 = -e^{2\nu(r)} dt^2 + e^{2\lambda(r)} dr^2 + r^2(d\theta^2 + \sin^2\theta d\phi^2). \quad (15)$$

Using Eq. (15) in Eq. (9), we obtain the form of non-metricity scalar as:

$$Q = -\frac{2e^{-2\lambda(r)}}{r} \left(2\nu'(r) + \frac{1}{r} \right), \quad (16)$$

where, the prime denotes the derivative with respect to the radial co-ordinate (r) and, interestingly, Q relies on the mathematical structure where the parallel transport, around any closed loop or in the Q -geometry, has no rotations or distortions. In other words, Q is based upon null coefficients of affine connections. Now, the anisotropic perfect fluid distribution is characterised as:

$$T_{ij} = (\rho + p_t)u_i u_j + p_t g_{ij} + (p_r - p_t)v_i v_j, \quad (17)$$

where, u_i represents the four velocity related to the anisotropic perfect fluid and v_i is the unit space-like vector in the radial direction. These parameters obey the relations $u^i u_i = -1$ and $v^i v_i = 1$. Moreover, ρ , p_r , p_t are the energy density and radial and tangential pressures, respectively, and are directed towards u_i and v_i . The electromagnetic energy-momentum tensor takes the form:

$$E_{ij} = \frac{1}{4\pi} \left(F_i^\eta F_{j\eta} - \frac{1}{4} g_{ij} F_{\zeta\eta} F^{\zeta\eta} \right). \quad (18)$$

Here, $F_{\zeta\eta}$ represents the Faraday-Maxwell tensor of the form, $F_{\zeta\eta} = \partial_\zeta A_\eta - \partial_\eta A_\zeta$, where $A_{\zeta\eta}$ represents the electromagnetic four potential. The fundamental Maxwell equations governing electromagnetism are represented as:

$$(\sqrt{-g} F^{ij})_{,j} = 4\pi J^i \sqrt{-g}, \quad F_{[ij,\delta]} = 0. \quad (19)$$

In the above expression, $J^i = \sigma u^i$, represents the electric four current, and σ defines the electric charge density. Following, Maxwell's equations, the strength of the electric field is expressed as:

$$E(r) = \frac{e^{\nu+\lambda}}{r^2} q(r), \quad (20)$$

where, $q(r)$ is the total charge contained within the sphere of radius r and is written as:

$$q(r) = 4\pi \int_0^r \sigma r'^2 e^\lambda dr'. \quad (21)$$

Conversely, the charge density can be written as:

$$\sigma = \frac{e^{-\lambda} \frac{dq(r)}{dr}}{4\pi r^2}. \quad (22)$$

For this study, we have considered a particular form of charge as follows [59]:

$$q = q_0 r^3, \quad (23)$$

where, q_0 is the intensity of charge and $q_0 = 0$ describes a neutral uncharged case.

Following the equation of motion given in Eq. (12) along with the anisotropic perfect fluid distribution of Eq. (17), we obtain a tractable set of the non-zero components of the Einstein-Maxwell field equations as follows:

$$\frac{f(Q)}{2} - f_Q \left[Q + \frac{1}{r^2} + \frac{2e^{-2\lambda}}{r} (\nu' + \lambda') \right] = 8\pi\rho + \frac{q^2}{r^4}, \quad (24)$$

$$-\frac{f(Q)}{2} + f_Q \left[Q + \frac{1}{r^2} \right] = 8\pi p_r - \frac{q^2}{r^4}, \quad (25)$$

$$-\frac{f(Q)}{2} + f_Q \left[\frac{Q}{2} - e^{-2\lambda} \left\{ \nu'' + 2 \left(\frac{\nu'}{2} + \frac{1}{2r} \right) (\nu' - \lambda') \right\} \right] = 8\pi p_t + \frac{q^2}{r^4}, \quad (26)$$

$$\frac{\cot\theta}{2} Q' f_{QQ} = 0, \quad (27)$$

where, $(')$ denotes derivatives with respect to r . Now, Eq. (27) is utilised to obtain the form of linear $f(Q)$ action and is expressed as:

$$f(Q) = \alpha_0 + \alpha_1 Q, \quad (28)$$

where, α_0 has the dimension of Km^{-2} and α_1 is dimensionless. Now, using Eqs. (24, 25, 26, 27, 28), the field equations in the modified $f(Q)$ theory of gravity reduce to an exact set of formulations in the following form:

$$\frac{1}{2r^2} \left[r^2 \alpha_0 - 2\alpha_1 e^{-2\lambda} (2r\lambda' - 1) - 2\alpha_1 \right] = 8\pi\rho + \frac{q^2}{r^4}, \quad (29)$$

$$\frac{1}{2r^2} \left[-r^2 \alpha_0 - 2\alpha_1 e^{-2\lambda} (2r\nu' + 1) + 2\alpha_1 \right] = 8\pi p_r - \frac{q^2}{r^4}, \quad (30)$$

$$\frac{e^{-2\lambda}}{2r} \left[-r\alpha_0 e^{2\lambda} - 2r\alpha_1 \nu'' - 2\alpha_1 (r\nu' + 1)(\nu' - \lambda') \right] = 8\pi p_t + \frac{q^2}{r^4}. \quad (31)$$

Since, the components of gravitational field equations depend on the metric potentials, $\lambda(r)$ and $\nu(r)$, we must remember a subtlety, in choosing the forms of $\lambda(r)$ and $\nu(r)$, as proposed by Lake [60] which states that $\lambda(r)$ must be finite and constant at the centre ($r = 0$) and must hold the following properties: $\lambda'(0) = 0$ and $\lambda''(0) > 0$. On the other hand, near the core, $\nu(r)$ must have the form $\nu = 1 + O(r^2)$, and it must increase towards the stellar boundary. This behaviour of the metric potentials, $\lambda(r)$ and $\nu(r)$ guarantees a monotonically decreasing energy density and pressure profile, with the maximum values concentrated in the core and diminishing steadily towards the surface. This characteristic is crucial for a stable and physically realistic stellar system. To fulfil the specified constraints in the present model, we opt for the Krori-Barua (KB) metric ansatz [61] in the form $\lambda = Ar^2$ and $\nu = Br^2 + C$. Now, plugging the metric potentials along with Eq. (23) in the set of equations Eqs. (29), (30) and (31), we obtain the non-zero components of the field equations as:

$$\rho = \frac{2\alpha_1 e^{-2Ar^2} - 2q_0^2 r^4 - 2\alpha_1 - r^2(8A\alpha_1 e^{-2Ar^2} - \alpha_0)}{16\pi r^2}, \quad (32)$$

$$p_r = \frac{-2\alpha_1 e^{-2Ar^2} + 2q_0^2 r^4 + 2\alpha_1 + r^2(8A\alpha_1 e^{-2Ar^2} - \alpha_0)}{16\pi r^2}, \quad (33)$$

$$p_t = \frac{e^{-2Ar^2}(4A\alpha_1 - \alpha_0 e^{2Ar^2} - 2q_0^2 r^2 e^{2Ar^2} - 8B\alpha_1 + 8ABr^2\alpha_1 - 8B^2 r^2\alpha_1)}{16\pi}. \quad (34)$$

The pressure anisotropy parameter (Δ) is expressed as:

$$\Delta = p_t - p_r. \quad (35)$$

Now, the total active gravitational mass contained within the sphere of radius R is,

$$m(r) = 4\pi \int_0^R \left(\rho + \frac{q^2}{8\pi r^4} \right) r^2 dr. \quad (36)$$

4. Boundary conditions

In the framework of modified theories of gravity, the equations of motion as prescribed by GR are modified. Therefore, the associated boundary conditions applicable to any stellar system in GR require suitable modifications [62]. Now, in the 4-dimensional spacetime manifold (Ω), there exist two distinct regions, *viz.*, the interior and exterior space-times. These regions are demarcated by a 3-dimensional hypersurface (Σ) defined by the induced metric h_{ij} in the X^i coordinate system, with indices excluding the direction orthogonal to Σ . We express the projection tensors and the normal vector from Ω and Σ in the form, $e_i^a = \frac{\partial x^a}{\partial X^i}$ and $n_a = \epsilon \delta_a \ell$, where, the affine connection in the perpendicular direction to Σ is denoted by ℓ and for the respective timelike, null and spacelike geodesics, ϵ takes the values -1 , 0 or 1 . In light of the above composition, one considers $n^a e_a^i = 0$. Now, the induced metric h_{ij} and extrinsic curvature tensor K_{ij} at the hypersurface are written in the form:

$$h_{ij} = e_i^a e_j^b g_{ab}, \quad K_{ij} = e_i^a e_j^b \nabla_a n_b. \quad (37)$$

In the framework of the distribution formalism introduced by Rosa et al. [63], one considers $[h_{ij} = 0]$, which reflects the continuity of the induced metric at Σ . However, to determine the constants appearing in the metric potentials, we must ensure that the extrinsic curvature tensor is also continuous at the junction. In the absence of a thin shell, the continuity of the extrinsic curvature tensor is written as $[K_{ij} = 0]$ [63]. Now, to compute the extrinsic curvature, we begin by considering the vacuum charged exterior Reissner-Nordström [64, 65] solution expressed as:

$$ds^2 = -\left(1 - \frac{2M}{r} + \frac{Q^2}{r^2}\right) dt^2 + \frac{dr^2}{\left(1 - \frac{2M}{r} + \frac{Q^2}{r^2}\right)} + r^2(d\theta^2 + \sin^2\theta d\phi^2), \quad (38)$$

where $M = m(r = R)$ and $Q = q(r = R)$ are the total mass and charge of the stellar configuration respectively. Interestingly, in the parametric space of spherically symmetric space-time, K_{ij}^\pm contains only two components *viz.*, K_{00} and $K_{\theta\theta} = K_{\phi\phi} \sin^2\theta$, where the $(+)$ and $(-)$ signs are for the exterior and interior space-time respectively. Using the KB ansatz and Eq. (38), we obtain the following components:

$$K_{00}^+ = \frac{-M - 2q_0^2 r^5}{r^2 \sqrt{\frac{r}{r - 2M + q_0^2 r^5}}}, \quad K_{00}^- = -2Bre^{-Ar^2 + 2Br^2 + 2C}, \quad (39)$$

$$K_{\theta\theta}^+ = \frac{r}{\sqrt{\frac{r^2}{Q^2 - 2Mr + r^2}}}, \quad K_{\theta\theta}^- = re^{-Ar^2}. \quad (40)$$

Another necessary condition is the nullification of radial pressure at the boundary, i.e.,

$$p_r(r = R) = 0. \quad (41)$$

Now, matching the extrinsic curvature tensors written in Eqs. (39) and (40) at the stellar boundary ($r = R$) and using Eq. (41), we obtain:

$$A = \frac{\ln\left[\frac{R^2}{R^2 - 2MR + Q^2}\right]}{2R^2}, \quad (42)$$

$$B = \frac{2q_0^2 R^6 - \alpha_0 R^4 - 2\alpha_1 Q^2 + 4\alpha_1 MR}{8\alpha_1 R^2 (Q^2 - 2MR + R^2)}, \quad (43)$$

$$C = \frac{1}{2} \left(\frac{4M\alpha_1 - \alpha_0 R^3 - 2q_0^2 R^5 (\alpha_1 - 1)}{8M\alpha_1 - 4R\alpha_1 (q_0^2 R^4 + 1)} \right) + \ln\left[\frac{R}{R - 2M + q_0^2 R^5}\right] + \ln\left[-\frac{4\alpha_1 (M + 2q_0^2 R^5)(R - 2M + q_0^2 R^5)^2}{\alpha_0 R^5 + 2q_0^2 R^7 (\alpha_1 - 1) - 4MR^2 \alpha_1}\right]. \quad (44)$$

5. Physical characteristics of the proposed model

Assessing the physical viability of the model is crucial to ensure that the compact star is physically realistic. A stellar model must comply with the regularity and reality conditions persistent in the context of relativistic stellar modeling to qualify as a compact star. In this section, we have considered the compact star PSR J0740+6620 with a mass of $2.072 M_\odot$ and radius of 12.39 Km [72] to study the impact of charge on various stellar parameters and to test the physical viability of the present theoretical model within the framework of modified $f(Q)$ gravity. Notably, following the study of Maurya et al. [67], we have considered $\alpha_0 = 10^{-46} \text{ Km}^{-2}$ along with $\alpha_1 = -0.5$.

5.1. Thermodynamic properties: energy density, radial and tangential pressures and pressure anisotropy

To ensure a realistic stellar model, the energy density and pressure profiles must have a monotonically decreasing nature. Moreover, for a physically acceptable solution, the condition of tangential pressure states that it must be positive throughout the interior of the compact star. The anisotropy in pressure, must be zero at the centre, i.e., $\Delta = 0$, which reflects that $p_r = p_t$ at the stellar core. These claims are supported by Figs. 1, 2, 3 and 4. From Figs. 1, 2

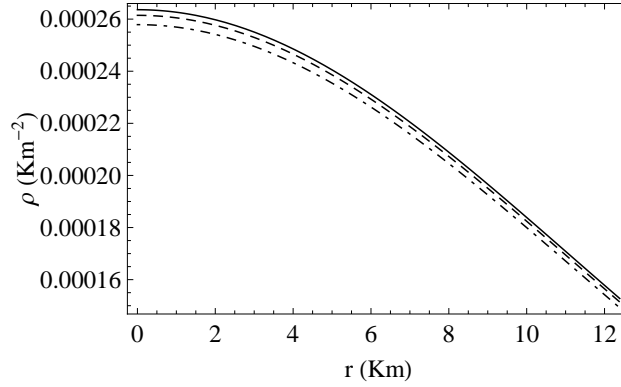


Figure 1: Radial variation of energy density (ρ) for different charge intensities (q_0). The solid, dashed and dot-dashed lines represent $q_0 = 0.0002, 0.0004$ and 0.0006 respectively.

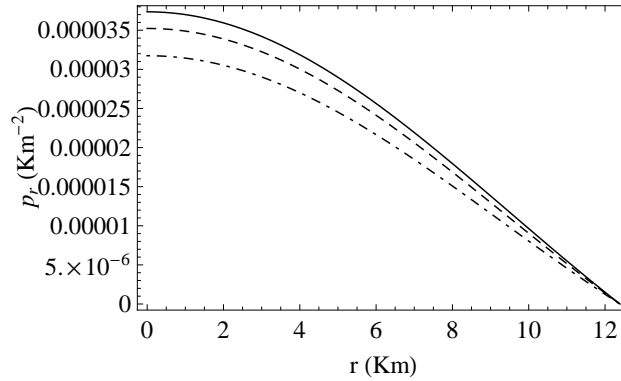


Figure 2: Radial variation of radial pressure (p_r) for different charge intensities (q_0). The solid, dashed and dot-dashed lines represent $q_0 = 0.0002, 0.0004$ and 0.0006 respectively.

and 3, it is noted here that, the energy density (ρ), radial (p_r) and tangential pressures (p_t) attain a maximum value at the stellar core, and as the charge increases, these physical parameters decrease. The maximisation of the core density and pressure profiles is ensured by $\rho'(0) = 0$, $p_r'(0) = 0$ and $p_t'(0) = 0$, while the nature of the gradients is negative for all $0 < r \leq R$. These behaviours of the gradients are shown in Figs. (5), (6) and (7). Moreover, Fig. (4) shows that $\Delta > 0$ throughout the interior of the star, which denotes a repulsive nature pointing towards a more massive structure.

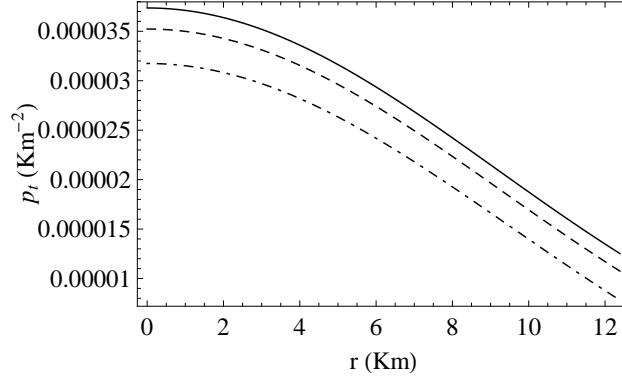


Figure 3: Radial variation of tangential pressure (p_t) for different charge intensities (q_0). The solid, dashed and dot-dashed lines represent $q_0 = 0.0002$, 0.0004 and 0.0006 respectively.

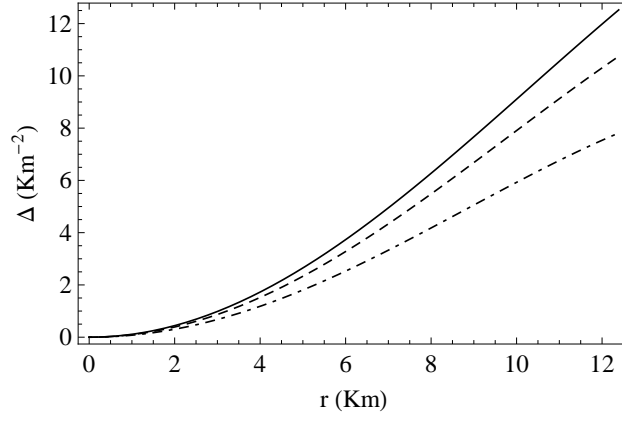


Figure 4: Radial variation of pressure anisotropy ($\Delta \times 10^6$) for different charge intensities (q_0). The solid, dashed and dot-dashed lines represent $q_0 = 0.0002$, 0.0004 and 0.0006 respectively.

In light of the above physical analysis, we can say that the thermodynamic properties are well satisfied in this model, which points towards a physically acceptable stellar model in stable equilibrium.

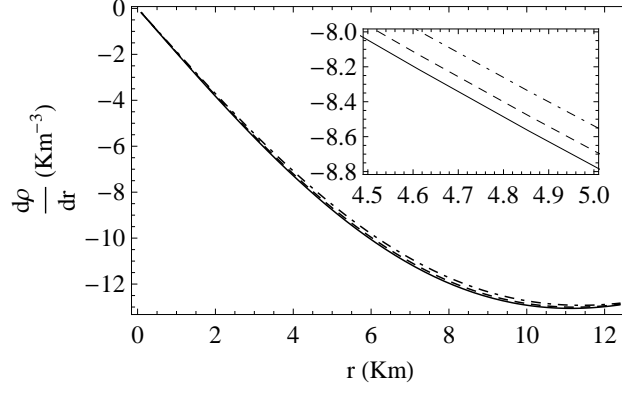


Figure 5: Radial variation of energy density gradient ($\frac{d\rho}{dr} \times 10^6$) for different charge intensities (q_0). The solid, dashed and dot-dashed lines represent $q_0 = 0.0002, 0.0004$ and 0.0006 respectively.

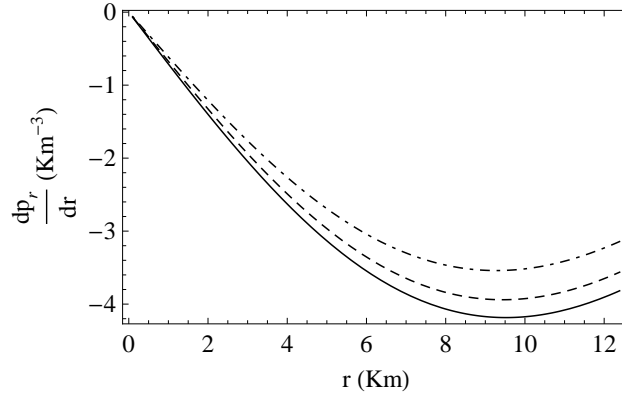


Figure 6: Radial variation of radial pressure gradient ($\frac{dp_r}{dr} \times 10^6$) for different charge intensities (q_0). The solid, dashed and dot-dashed lines represent $q_0 = 0.0002, 0.0004$ and 0.0006 respectively.

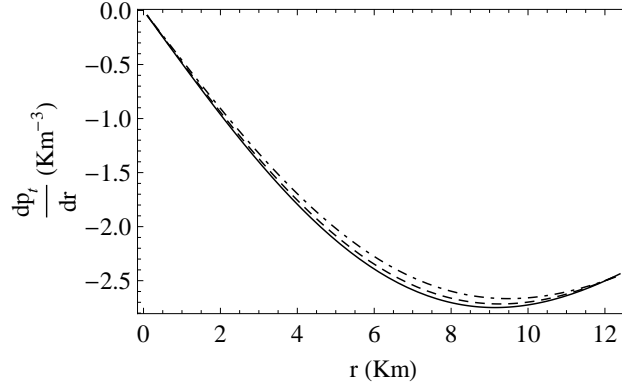


Figure 7: Radial variation of tangential pressure gradient ($\frac{dp_t}{dr} \times 10^6$) for different charge intensities (q_0). The solid, dashed and dot-dashed lines represent $q_0 = 0.0002, 0.0004$ and 0.0006 respectively.

5.2. Maximum mass and radius from TOV equation

In this section, we numerically solve the TOV equations [68, 69] to obtain the maximum mass and radius for a charged compact star. It should be noted that, the solution of the TOV equation is entirely based upon the choice of

a particular EoS. Hence, to resort to a suitable EoS, we adopt the method of maximising the radial sound velocity ($v_r^2 = \frac{dp_r}{d\rho} = 1$), to the extreme end of causality, at the centre and the method of curve fitting from the data set of ρ and p_r . We tabulate the EoS for increasing charge intensity (q_0) in Table 1. Using Table 1, we have numerically

Table 1: Best fit EoS with increasing charge intensity	
Charge intensity (q_0)	EoS
0.0002	$p_r = 0.910646 \rho - 0.000354486$
0.0004	$p_r = 0.910245 \rho - 0.000354205$
0.0006	$p_r = 0.909595 \rho - 0.000353745$

solved TOV equations and the results are plotted in Fig. 8. The obtained maximum mass and radius are tabulated in Table 2. From Table 2, it is evident that the increase in charge intensity (q_0) results in an increase in the maximum

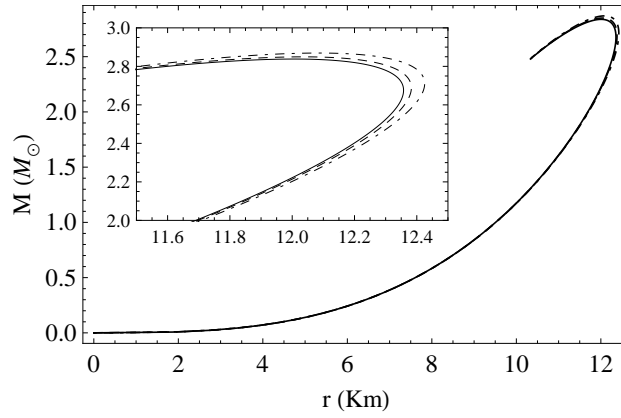


Figure 8: Mass-radius plot for different charge intensities (q_0). The solid, dashed and dot-dashed lines represent $q_0 = 0.0002$, 0.0004 and 0.0006 respectively.

Table 2: Maximum mass and radius from TOV equation		
Charge intensity (q_0)	Maximum mass (M_\odot)	Radius (Km)
0.0002	2.838	12.0039
0.0004	2.849	12.0348
0.0006	2.869	12.0822

mass in the present scenario, which denotes the transition of the EoS from a softer to a stiffer nature. Interestingly, in this section, we have predicted the radii of some recently observed pulsars and GW events and evaluated their physical characteristic parameters, *viz.*, central density (ρ_c), surface density (ρ_s) and central pressure (p_c), and they are tabulated in Table 3.

Table 3: Tabulation of radius prediction and physical parameters

Compact Object	Measured mass (M_\odot)	Measured radius (Km)	Charge intensity (q_0)	Predicted radius (Km)	Central density (ρ_c)	Surface density (ρ_s)	Central pressure (p_c)
GW 190814 [70]	$2.59^{+0.08}_{-0.09}$	—	0.0006	11.82	0.41×10^{15}	0.23×10^{15}	0.52×10^{35}
PSR J0952-0607 [71]	$2.35^{+0.17}_{-0.17}$	—	0.0002	12.15	0.46×10^{15}	0.23×10^{15}	0.78×10^{35}
PSR J0740+6620 [72]	$2.072^{+0.067}_{-0.066}$	$12.39^{+1.30}_{-0.98}$	0.0006	11.82	0.41×10^{15}	0.23×10^{15}	0.52×10^{35}
4U 1820-30 [73]	$1.58^{+0.06}_{-0.06}$	$9.1^{+0.4}_{-0.4}$	0.0002	10.94	0.37×10^{15}	0.24×10^{15}	0.37×10^{35}
EXO 1745-248 [74]	1.4	11	0.0006	10.59	0.35×10^{15}	0.23×10^{15}	0.27×10^{35}
HER X-1 [75]	$0.85^{+0.15}_{-0.15}$	$8.1^{+0.41}_{-0.41}$	0.0002	9.05	0.32×10^{15}	0.24×10^{15}	0.17×10^{35}

5.3. Causality condition

In the pursuit of a realistic model for an anisotropic compact star, a valuable approach for characterising the dense interior matter lies in the investigation of sound wave velocities. The radial and tangential sound velocities are expressed as $v_r^2 = \frac{dp_r}{d\rho}$ and $\frac{dp_t}{d\rho}$, respectively, where ρ , p_r and p_t are the energy density, and radial and tangential pressures, respectively. In this particular formulation, we have used the system of units $\hbar = c = 1$, and the causality criterion imposes an absolute upper bound of the sound velocities as $v_r^2 \leq 1$ and $v_t^2 \leq 1$. However, the thermodynamic equilibrium ensures that $v_r^2 > 0$ and $v_t^2 > 0$. Hence, the combined effects of both conditions, i.e., $0 < v_r^2 \leq 1$ and $0 < v_t^2 \leq 1$, must be simultaneously satisfied within the stellar configuration. To circumvent the mathematical intricacies, we have opted to represent the radial variation of sound velocities graphically in Figs. 9 and 10. It is

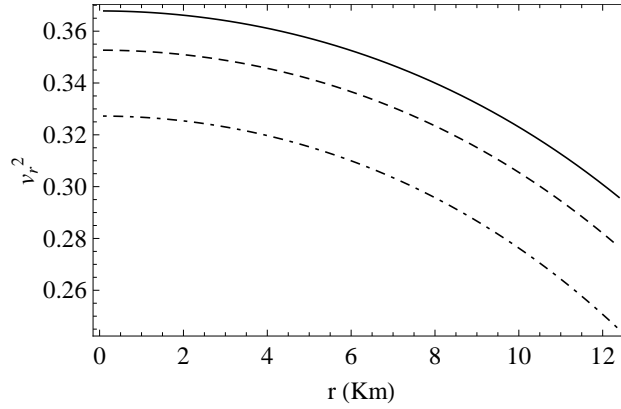


Figure 9: Radial variation of radial sound velocity (v_r^2) for different charge intensities (q_0). The solid, dashed and dot-dashed lines represent $q_0 = 0.0002$, 0.0004 and 0.0006 respectively.

evident here that the causality conditions are well maintained within the stellar interior.

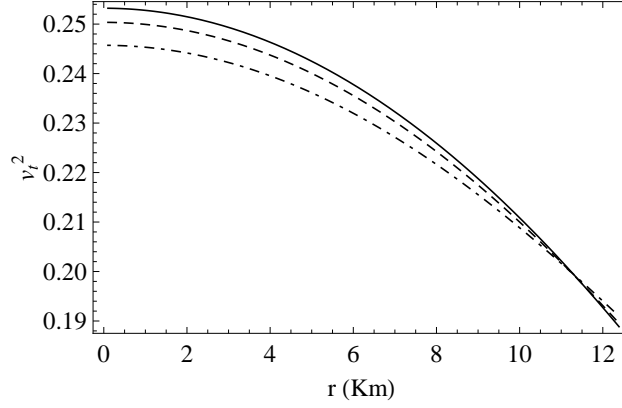


Figure 10: Radial variation of tangential sound velocity (v_t^2) for different charge intensities (q_0). The solid, dashed and dot-dashed lines represent $q_0 = 0.0002, 0.0004$ and 0.0006 respectively.

5.4. Energy conditions

In the field of gravitational theory, constraints known as energy conditions are applied to matter distributions. These constraints are essential for deriving a physically feasible energy-momentum tensor. Essentially, these conditions provide a method to explore the characteristics of matter distribution without requiring detailed information about the intrinsic matter content. Therefore, it is feasible to discern the physical characteristics of extreme phenomena, such as gravitational collapse or the presence of a geometrical singularity, without explicit knowledge of energy density or pressure. Essentially, the examination of energy conditions is an algebraic issue [76], more precisely, it is an eigenvalue problem associated with the energy-momentum tensor. In a 4D spacetime, the investigation of energy conditions results in the roots of a quartic polynomial, a process that becomes complex due to the existence of analytical solutions for eigenvalues. Although finding a general solution can be challenging, a physically plausible fluid distribution should simultaneously adhere to the null, weak, strong, and dominant energy conditions [76, 77, 78] within the confines of the stellar boundary. In this study, we have examined the energy conditions [79, 80] for the current stellar configuration in the following form:

$$\begin{aligned}
 NEC : \rho + \frac{q^2}{8\pi r^4} &\geq 0, \\
 WEC : \rho + p_r &\geq 0, \rho + p_t + \frac{q^2}{4\pi r^4} \geq 0, \\
 SEC : \rho + p_r + 2p_t + \frac{q^2}{4\pi r^4} &\geq 0, \\
 DEC : \rho - p_r + \frac{q^2}{4\pi r^4} &\geq 0, \rho - p_t \geq 0.
 \end{aligned}$$

From Fig. 11, we note that all the necessary energy conditions are satisfactorily obeyed throughout the stellar interior.

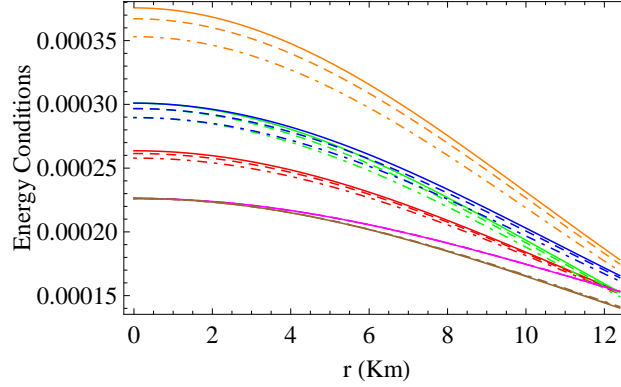


Figure 11: Radial variation of energy conditions for different charge intensities (q_0). Here, Red, Green, Blue, Orange, Magenta and Brown lines represent $(\rho + \frac{q^2}{8\pi r^4})$, $(\rho + p_r)$, $(\rho + p_t + \frac{q^2}{4\pi r^4})$, $(\rho + p_r + 2p_t + \frac{q^2}{4\pi r^4})$, $(\rho - p_r + \frac{q^2}{4\pi r^4})$ and $(\rho - p_t)$ respectively. The solid, dashed and dot-dashed lines represent $q_0 = 0.0002$, 0.0004 and 0.0006 respectively.

6. Stability analysis

The stability of this model is examined using the following methodologies:

- Generalised TOV equation
- Herrera cracking condition
- Adiabatic index
- Zel'dovich condition

6.1. Generalised TOV equation

Examining the stability of a model subjected to various forces is essential. For an anisotropic charged compact object, this stability analysis focuses on four force components: (i) the gravitational force (F_g), (ii) the hydrostatic force (F_h), (iii) the anisotropic force (F_a), and (iv) the electromagnetic force (F_q). To ensure that the model remains in stable equilibrium, the combined effects of these forces must be balanced. In this study, to analyse the stability, we utilise the generalised form of the Tolman–Oppenheimer–Volkoff (TOV) equation [68, 69], as expressed below:

$$-\frac{M_G(\rho + p_r)}{r^2}e^{\lambda-\nu} - \frac{dp_r}{dr} + \frac{2\Delta}{r} + \frac{q}{4\pi r^4} \frac{dq}{dr} = 0, \quad (45)$$

where, M_G is demarcated as the active gravitational mass obtained from the Tolman-Whittaker mass formula [81] in the following form:

$$M_G(r) = r^2 \nu' e^{\nu-\lambda}. \quad (46)$$

Substituting Eq. (46) into Eq. (45), we obtain:

$$-\nu'(\rho + p_r) - \frac{dp_r}{dr} + \frac{2\Delta}{r} + \frac{2\Delta}{r} + \frac{q}{4\pi r^4} \frac{dq}{dr} = 0. \quad (47)$$

Here,

$$F_g = -\nu'(\rho + p_r), \quad (48)$$

$$F_h = -\frac{dp_r}{dr}, \quad (49)$$

$$F_a = \frac{2\Delta}{r}, \quad (50)$$

$$F_q = \frac{q}{4\pi r^4} \frac{dq}{dr}. \quad (51)$$

By utilising Eqs. (32), (33) and (34) in Eqs. (48), (49), (50) and (51), we obtain the equilibrium condition prescribed in the generalised TOV equations. To avoid the mathematical complexity, we have shown the condition of stable equilibrium through a graphical representation. Fig. 12 shows that our model is stable under the influence of different forces.

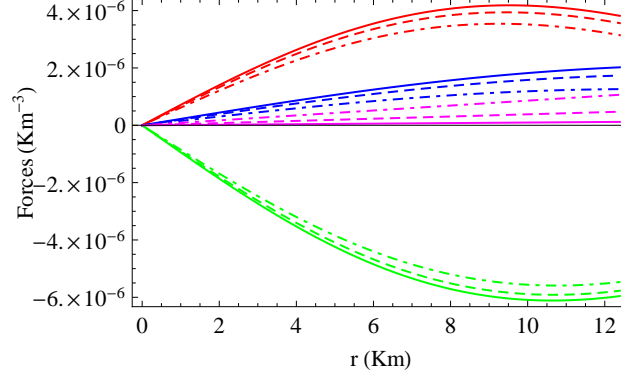


Figure 12: Radial variation of different forces for different charge intensities (q_0). Here, Green, Red, Blue and Magenta and Brown lines represent F_g , F_h , F_a and F_q respectively. The solid, dashed and dot-dashed lines represent $q_0 = 0.0002$, 0.0004 and 0.0006 respectively.

6.2. Herrera cracking condition

According to Herrera's work [82], the concept of “Cracking” or “Breaking” in the context of a self-gravitating compact object refers to the appearance of total radial forces in various regions of the spherical structure, each with different signs, when perturbations are introduced into the system. If the EoS is taken into account, cracking can arise from two scenarios, namely, i) a local anisotropic fluid, or ii) a slowly contracting and radiating perfect fluid. Utilising this cracking condition, Abreu et al. [83] explored the impact of local anisotropy on the distribution of local anisotropic fluid. They demonstrated that when perturbations exist in the system, potential stability can be established through the difference between the squares of radial (v_r^2) and tangential (v_t^2) sound velocities expressed as:

$$0 \leq |v_r^2 - v_t^2| \leq 1. \quad (52)$$

A stellar model that adheres to this relation is referred to as a stable structure. From Fig. (13), we note that the Abreu inequality is well maintained throughout the interior of the stellar configuration.

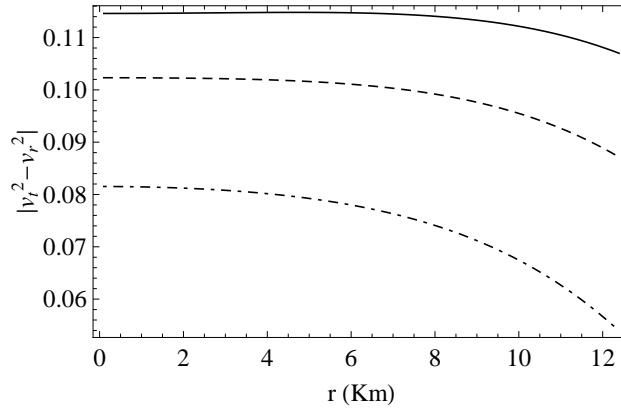


Figure 13: Radial variation of $|v_r^2 - v_t^2|$ for different charge intensities (q_0). The solid, dashed and dot-dashed lines represent $q_0 = 0.0002$, 0.0004 and 0.0006 respectively.

6.3. Adiabatic index

The adiabatic index (Γ) is the ratio of two specific heats that signify the rigidity of the EoS at a particular density. In the context of a relativistic anisotropic stellar structure, the adiabatic index is represented as:

$$\Gamma = \frac{\rho + p_r}{p_r} \frac{dp_r}{dr} = \frac{\rho + p_r}{p_r} v_r^2. \quad (53)$$

According to Heintzmann and Hillebrandt [84], a Newtonian matter distribution demonstrates, $\Gamma > \frac{4}{3}$. Later, Chan et al. [85] extended the upper bound of the adiabatic index considering the existence of pressure anisotropy, and it is articulated as follows:

$$\Gamma > \Gamma'_{max}, \quad (54)$$

where,

$$\Gamma'_{max} = \frac{4}{3} - \left[\frac{4}{3} \frac{(p_r - p_t)}{|p'_r| r} \right]_{max}. \quad (55)$$

Now, to determine the anisotropic limit, we have evaluated Γ'_{max} for different charge intensities (q_0) and the composite results are plotted in Fig. 14.

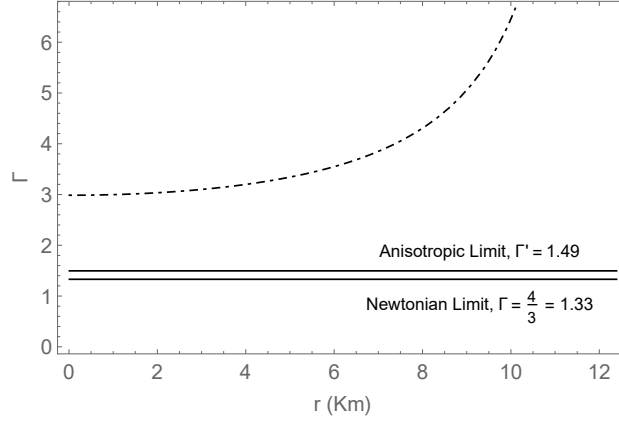


Figure 14: Radial variation of adiabatic index (Γ) for different charge intensities (q_0). The solid, dashed and dot-dashed lines represent $q_0 = 0.0002$, 0.0004 and 0.0006 respectively.

6.4. Zel'dovich condition

Based on the Zel'dovich condition [86, 87, 88, 89], a stellar structure is considered stable if the ratio of pressure to density is less than one throughout the entire structure. If we denote this ratio as Ω , then considering the radial (p_r) and tangential (p_t) pressures, we obtain $\Omega_r = \frac{p_r}{\rho}$, and $\Omega_t = \frac{p_t}{\rho}$. The criterion for stability is that Ω_r and Ω_t must be less than 1. It is evident from Figs. 15 and 16 that the Zel'dovich criterion is well maintained within the stellar interior. Hence, the present model can be termed a stable configuration.

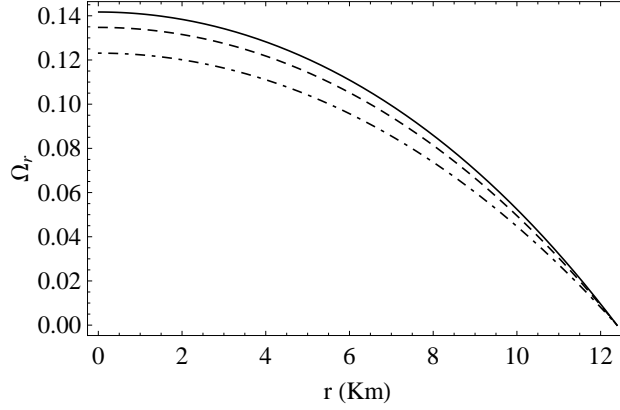


Figure 15: Radial variation of (Ω_r) for different charge intensities (q_0). The solid, dashed and dot-dashed lines represent $q_0 = 0.0002, 0.0004$ and 0.0006 respectively.

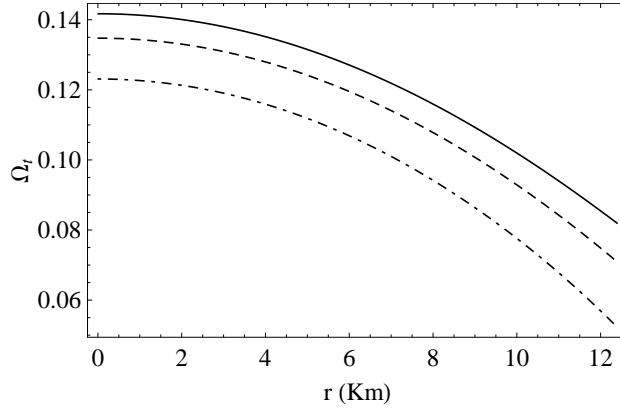


Figure 16: Radial variation of adiabatic index (Ω_t) for different charge intensities (q_0). The solid, dashed and dot-dashed lines represent $q_0 = 0.0002, 0.0004$ and 0.0006 respectively.

7. Discussion

Finally, we summarise the major findings of the present paper and our efforts to mimic a charged compact stellar structure in the framework of symmetric teleparallel $f(Q)$ gravity. Taking into account a spherically symmetric space-time, we combine the KB metric ansatz [61], with a linear form of the $f(Q)$ action, which allows us to formulate a singularity-free solution of the Einstein-Maxwell field equations within the framework of $f(Q)$ theory. This solution incorporates a specific form of charge, denoted as $q(r) = q_0 r^3$, as outlined in Eq. (23), where q_0 is the charge intensity and $q_0 = 0$ illustrates an uncharged stellar configuration.

Within this theoretical construct, we have selected PSR J0740+6620 [72] as a potential candidate for a charged compact star. We analyse and represent our results, both numerically and graphically, by varying the charge intensity (q_0). It has been shown in Refs. [62, 63] that the modified theories of gravity lead to alterations in the boundary conditions of GR. This paper addresses these changes by assessing the continuity of both the induced metric and the extrinsic curvature tensors at the boundary of the stellar structure. We have used, i) the matching of interior solutions with the Reissner-Nordström [64, 65] exterior to compute the extrinsic curvature tensors, as obtained in Eqs. (39) and (40), and ii) the condition of nullification of radial pressure at the stellar boundary, to compute the necessary constant present in the model. We have noted the following key characteristic features:

- Radial variation of the thermodynamic properties of a stellar structure, such as the energy density (ρ), radial (p_r) and tangential (p_t) pressure profiles are represented in Figs. 1, 2, 3. As the charge intensity increases, the energy

density and pressure profiles decrease. However, the monotonically decreasing nature of the characteristic profiles is well preserved in this model. Furthermore, the radial variation of anisotropy is illustrated in Fig. 4. From Fig. 4, we note that, $\Delta > 0$, which indicates a repulsive anisotropic behaviour. This nature further indicates a more massive stellar structure. We also note that at the centre ($r \rightarrow 0$), $\Delta \rightarrow 0$, i.e., $p_r = p_t$, which is another viable condition in favour of stable compact star modeling. The radial variations of pressure and density gradients are negative, as shown in Figs. 5, 6 and 7, which aids in the maximisation of the core density. Hence, it may be concluded that the physical parameters are consistent throughout the stellar structure.

- Obtaining the maximum mass through TOV equations depends on the particular choice of the EoS. In the present scenario, we have obtained the suitable EoS by maximising the radial sound velocity at the stellar centre, i.e., $\frac{dp_r}{d\rho}|_{r=0} = 1$. Moreover, we have used the method of curve fitting to obtain the best fit EoS in this model, which are tabulated in Table 1 for increasing charge intensity (q_0). Using the EoS, we numerically evaluate the TOV equation, and Fig. 8 depicts the mass-radius plot. The maximum masses and radii for the increasing charge intensity are listed in Table 2. We show the predicted radii of different recently observed pulsars and GW 190814 in Table 3 and it is noted that our model complies with the observational results of compact star candidates.
- Figs. 9 and 10 show the variations of radial (v_r^2) and tangential (v_t^2) sound velocities with the radial distance. Notably, with increasing charge intensity, both v_r^2 and v_t^2 decrease within the stellar boundary. However, it is evident that both the velocities are well-regulated, as they do not surpass the speed of light and comply with the causality condition.
- In the framework of $f(Q)$ gravity and considering the presence of charge, we have studied the necessary and sufficient energy conditions for a well-behaved compact star model, which is demonstrated in Fig. (11). We note that, all the energy conditions are well maintained throughout the stellar structure.
- We have assessed the stability of the present model, within the charged $f(Q)$ formalism, using the generalised TOV approach, the cracking condition proposed by Herrera, the radial variation of the adiabatic index and the Zel'dovich criterion. Fig. 12 shows that the proposed model is in hydrostatic equilibrium under the impact of different forces and with the variation of charge intensity (q_0). To simulate a realistic stellar structure, perturbations must be considered within the system. With the presence of such perturbations, the potential stability of the charged model is obtained through the study of cracking condition, as proposed by Herrera. Fig. 13 shows that the cracking condition is well obeyed in this model. The modifications introduced in the adiabatic index due to the presence of anisotropy are written in Eq. (55) and the investigation of stability on the basis of the adiabatic index is shown in Fig. 14. Figs. 15 and 16 show that the Zel'dovich criterion is well satisfied throughout the charged stellar structure.

To sum up, it is fascinating to observe that the $f(Q)$ gravity facilitates the creation of physically plausible models that align with fundamental principles in the context of static, spherically symmetric space-times. Therefore, considering all the key aspects of the present model, we can evidently state that we have presented here a stable and physically acceptable singularity-free charged compact star model within the framework of the $f(Q)$ theory of gravity.

8. Acknowledgments

DB is thankful to DST, Govt. of India, for providing the fellowship vide no: DST/INSPIRE/03/2022/000001.

References

- [1] A.G. Riess et al., Astron. J. 116 (1998) 1009.
- [2] S. Perlmutter et al., Astrophys. J. 517 (1999) 565.
- [3] N. Suzuki et al., Astrophys. J. 746 (2012) 85.
- [4] H. Weyl, Ann. der Phys. 364 (1919) 101.
- [5] A. Einstein, Sitzber. Preuss. Akad. Wiss. 17 (1928) 217.
- [6] K. Hayashi, T. Shirafuji, Phys. Rev. D 19 (1979) 3524.

- [7] T. Sauer, *Historia Mathematica* 33 (2006) 399.
- [8] J.M. Nester, H.-J. Yo, *Chin. J. Phys.* 37 (1999) 113.
- [9] J.B. Jiménez, L. Heisenberg, T. Koivisto, *Phys. Rev. D* 98 (2018) 044048.
- [10] J.B. Jiménez, L. Heisenberg, T. Koivisto, *J. Cosmol. Astropart. Phys.* 2018 (2018b) 039.
- [11] L. Heisenberg, *Phys. Rep.* 796 (2019) 1.
- [12] M. Hohmann, C. Pfeifer, U. Ualikhanova, J.L. Said, *Phys. Rev. D* 99 (2019) 024009.
- [13] I. Soudi et al., *Phys. Rev. D* 100 (2019) 044008.
- [14] R. Lazkoz, F.S.N. Lobo, M. Ortiz-Banós, V. Salzano, *Phys. Rev. D* 100 (2019) 104027.
- [15] F. D' Ambrosio et al., *Phys. Rev. D* 105 (2022) 024042.
- [16] F. D' Ambrosio, S.D.B. Fell, L. Heisenberg, S. Kuhn, *Phys. Rev. D* 105 (2022) 024042.
- [17] F. Bajardi, D. Vernieri, S. Capozziello, *Eur. Phys. J. Plus* 135 (2020) 912.
- [18] W. Khylllep, A. Paliathanasis, J. Dutta, *Phys. Rev. D* 103 (2021) 103521.
- [19] I. Ayuso, R. Lazkoz, V. Salzano, *Phys. Rev. D* 103 (2021) 063505.
- [20] L. Heisenberg, *arXiv:2309.15958v1*.
- [21] B.J. Barros, T. Barreiro, T. Koivisto, N.J. Nunes, *Phys. Dark Universe* 30 (2020) 100616.
- [22] J.B. Jiménez, L. Heisenberg, T. Koivisto, S. Pekar, *Phys. Rev. D* 101 (2020) 103507.
- [23] F.K. Anagnostopoulos, S. Basilakos, E.N. Saridakis, *Phys. Lett. B* 822 (2021) 136634.
- [24] K. Flathmann, M. Hohmann, *Phys. Rev. D* 103 (2021) 044030.
- [25] F. D' Ambrosio, L. Heisenberg, S. Zentarra, *arXiv:2308.02250v1*.
- [26] H. Cromartie et al., *Nat. Astron.* 4 (2020) 72.
- [27] R. Kippenhahn, A. Weigert, *Stellar Structure and Evolution* (Springer, Berlin, 1990).
- [28] R.A. Broglia, V. Zelevinsky (eds.), *Fifty Years of Nuclear BCS: Pairing in Finite Systems* (World Scientific Publishing Co. Pte. Ltd., Singapore, 2013).
- [29] D. Page, J.M. Lattimer, M. Prakash, in *Novel Superfluids*, vol. 2, ed. by K.H. Bennemann, J.B. Ketterson (Oxford University Press, Oxford, 2014), p.505.
- [30] A.I. Sokolov, *JETP* 79 (1980) 1137.
- [31] R.F. Sawyer, *Phys. Rev. Lett.* 29 (1972) 382. [Erratum: *Phys. Rev. Lett.* 29 (1972) 823.].
- [32] L. Herrera, N.O. Santos, *Phys. Rep.* 286 (1997) 53.
- [33] S. Rosseland, *Mon. Not. R. Astron. Soc* 84 (1924) 720.
- [34] A.S. Eddington, *Internal Constitution of the stars* (Cambridge University Press, Cambridge, 1926).
- [35] B.V. Ivanov, *Phys. Rev. D* 65 (2002) 104001.
- [36] F. Hoyle, J.V. Narlikar, *Proc. Roy. Soc.* 278 (1964) 465.
- [37] W.B. Bonnor, *Mon. Not. R. Astron. Soc.* 129 (1965) 443.
- [38] R. Stettner, *Ann. Phys. (N. Y.)* 80 (1973) 212.
- [39] A. Krasinski, *Inhomogeneous Cosmological Models* (Cambridge University Press, Cambridge, 1997).
- [40] J.D. Bekenstein, *Phys. Rev. D* 4 (1971) 2185.
- [41] A. Saha et al., *Phys. Scr.* 98 (2023) 105012.
- [42] K.B. Goswami et al., *Eur. Phys. J. C.* 82 (2022) 1042.
- [43] A. Saha et al., *Pramana -J. Phys.* 97 (2023) 10.
- [44] A. Saha et al., *Chin. Phys. C.* 47 (2023) 015107.
- [45] D. Bhattacharjee, P.K. Chattopadhyay, *Phys. Scr.* 98 (2023) 085013.
- [46] N. Pradhan, N. Pant, *Astrophys. Space Sci.* 356 (2015) 67.
- [47] K.N. Singh, et al., *Int. J. Theo. Phys.* 54 (2014) 3408.
- [48] N. Pant et al., *Astrophys. Space Sci.* 355 (2015) 137.
- [49] S.K. Maurya et al., *Eur. Phys. J. C* 75 (2015) 389.
- [50] S. Kaur et al., *New Astronomy* 110 (2024) 102230.
- [51] S.K. Maurya et al., *Astrophys. J. Suppl. Ser.* 269 (2023) 35.
- [52] A. Errehymy et al., *Eur. Phys. J. Plus* 137 (2022) 1311.
- [53] S. V. Lohakare et al., *Mon. Not. R. Astron. Soc.* 526 (2023) 3796.
- [54] P. Bhar, A. Malik, A. Almas, *Chin. J. Phys.* 88 (2024) 839.
- [55] P. Bhar, J.M.Z. Pretel, *Phys. Dark Universe* 42 (2023) 101322.
- [56] P. Bhar, *Fortschritte der Physik* 71 (2023) 2300074.
- [57] M.Z. Gul et al., *Eur. Phys. J. C.* 84 (2024) 8.
- [58] D. Zhao, *Eur. Phys. J. C* 82 (2022) 303.
- [59] D.V.P. Gonçalves, L. Lazzari, *Phys. Rev. D* 102 (2020) 034031.
- [60] K. Lake, *Phys. Rev. D* 67 (2003) 104015.
- [61] K.D. Krori, J. Barua, *J. Phys. A: Math. Gen.* 8 (1975) 508.
- [62] J.L. Rosa, *Phys. Rev. D* 109 (2024) 064018.
- [63] J.L. Rosa, N. Ganiyeva, F.N.S. Lobo, *Eur. Phys. J. C* 83 (2023) 1040.
- [64] H. Reissner, *Ann. Phys.* 50 (1916) 106.
- [65] G. Nordström, *Verhandl. Koninkl. Ned. Akad. Wetenschap., Afdel. Natuurk.* 26 (1918) 1201.
- [66] T.E. Riley et al., *Astrophys. J. Lett.* 918 (2021) L27.
- [67] S.K. Maurya et al., *Astrophys. J. Suppl. Ser.* 269 (2023) 35.
- [68] R.C. Tolman, *Phys. Rev.* 55 (1939) 364.
- [69] J.R. Oppenheimer, G.M. Volkoff, *Phys. Rev.* 55 (1939) 374.

- [70] R. Abbott et al., *Astrophys. J. Lett.* 896 (2020) L44.
- [71] G.A. Carvalho et al., *Eur. Phys. J. C* 82 (2022) 1096.
- [72] T. E. Riley et al., *Astrophys. J. Lett.* 918 (2021) L27.
- [73] T. Güver et al., *Astrophys. J.* 719 (2010) 1807.
- [74] F. Özel, T. Güver, D. Psaltis, *Astrophys. J.* 693 (2009) 1775.
- [75] M. K. Abubekurov et al., *Astron.Rep.* 52 (2008) 379.
- [76] C.A. Kolassis, N.O. Santos, D. Tsoubelis, *Class. Quantum Gravity* 5 (1988) 1329.
- [77] S.W. Hawking, G.F.R. Ellis, *The Large Scale Structure of Space-time* (Cambridge University Press, Cambridge, 1973).
- [78] R. Wald, *General Relativity* (University of Chicago Press, Chicago, 1984).
- [79] B.P. Brassel, S.D. Maharaj, R. Goswami, *Entropy* 23 (2021) 1400.
- [80] B.P. Brassel, S.D. Maharaj, R. Goswami, *Prog. Theor. Exp. Phys.* 2021 (2021) 103E01.
- [81] Ø. Grøn, *Phys. Rev. D* 31 (1985) 2129.
- [82] L. Herrera, *Phys. Lett. A* 165 (1992) 206.
- [83] H. Abreu, H. Hernandez, L. A. Núñez, *Class. Quantum Gravity* 24 (2007) 4631.
- [84] H. Heintzmann, W. Hillebrandt, *Astron. Astrophys.* 38 (1975) 51.
- [85] R. Chan, L. Herrera, N.O. Santos, *Mon. Not. R. Astron. Soc.* 265 (1993) 533.
- [86] S.L. Shapiro, S.A. Teukolsky, *Black holes, white dwarfs, and neutron stars: The physics of compact objects* (John Wiley & Sons, 2008).
- [87] Y.B. Zel'dovich, I. D. Novikov, *Relativistic astrophysics. Vol.1: Stars and Relativity* (Chicago: University of Chicago Press, 1971).
- [88] Y.B. Zel'dovich, I. D. Novikov, J. Silk, *Physics Today* 25 (1972) 63.
- [89] Y.B. Zel'dovich, *J. Exp. Theor. Phys* 14 (1962) 1609.